

## Collective Dynamics of Complex Plasma Bilayers

P. Hartmann,<sup>1,2</sup> Z. Donkó,<sup>1,2</sup> G. J. Kalman,<sup>2</sup> S. Kyrkos,<sup>3</sup> K. I. Golden,<sup>4</sup> and M. Rosenberg<sup>5</sup>

<sup>1</sup>Research Institute for Solid State Physics and Optics of the Hungarian Academy of Sciences, H-1525 Budapest, P.O. Box 49, Hungary

<sup>2</sup>Department of Physics, Boston College, 140 Commonwealth Avenue, Chestnut Hill, Massachusetts 02467, USA

<sup>3</sup>Department of Chemistry and Physics, Le Moyne College, 1419 Salt Springs Road, Syracuse, New York 13214, USA

<sup>4</sup>Department of Mathematics and Statistics, College of Engineering and Mathematical Sciences, University of Vermont, Burlington, Vermont 05401-1455, USA

<sup>5</sup>Department of Electrical and Computer Engineering, University of California San Diego, La Jolla, California, 92093, USA

(Received 10 August 2009; published 9 December 2009)

A classical dusty plasma experiment was performed using two different dust grain sizes to form a strongly coupled asymmetric bilayer (two closely spaced interacting monolayers) of two species of charged dust particles. The observation and analysis of the thermally excited particle oscillations revealed the collective mode structure and dispersion (wave propagation) in this system; in particular, the existence of the theoretically predicted  $k = 0$  energy (frequency) gap was verified. Equilibrium molecular-dynamics simulations were performed to emulate the experiment, assuming Yukawa-type interparticle interaction. The simulations and analytic calculations based both on lattice summation and on the quasilocated charge approximation approach are in good agreement with the experimental findings and help in identifying and characterizing the observed phenomena.

DOI: 10.1103/PhysRevLett.103.245002

PACS numbers: 52.27.Lw, 52.35.-g

Particle bilayers (parallel planes occupied by interacting particles and separated by a distance comparable to the interparticle distance within the layers) can be viewed as an intermediate stage between two-dimensional (2D) and three-dimensional (3D) systems. It is the interplay of the 3D interaction and the 2D dynamics that creates the rich new physics predicted and observed in interacting bilayers that makes these systems interesting in their own right. At the same time, bilayer configurations are also ubiquitous in widely different physical systems. Of special importance are those of charged particles (with like charges, unipolar bilayer; with opposite charges, bipolar bilayer). Examples are semiconductor heterostructures [1], cryogenic traps [2], overdamped system of lipid membranes [3], interfacial superconductors [4], etc.

From the theoretical point of view, during the past three decades unipolar layered systems were studied in the weak coupling limit by means of analytic calculations [5,6] and in the strongly coupled regime by semianalytic lattice calculations [7], approximate liquid state calculations [8], and computer simulations [9–13]. More recently, bipolar (electron-hole) bilayers have been the focus of intense computer simulation efforts, both in the classical [14–16] and in the quantum regimes [17,18], where features such as structural phase transitions, bound dipole formation [19], etc. were detected.

Very recently a seminal observation by Hyde and co-workers [20] has led to the realization that strongly coupled unipolar bilayers can be created in laboratory complex (dusty) plasma environments. This can be accomplished by using a mixture of two differently sized grains: in view of their necessarily different charge to mass ( $Z/m$ ) ratios, the two species would settle at different equilibrium

heights in the plasma sheath, as governed by the local balance of gravitational and electric forces. Thus this novel type of bilayer would be, in contrast to most of the previously observed ones, a binary bilayer with hitherto unexplored features. Its structural properties were already reported in [20]. Subsequent computer simulations predicting collective excitations (wave propagation) and their dispersion were carried out in recent years both for Coulomb- and Yukawa-type isotropic interactions [21,22].

In this Letter we report on the experimental investigation of the collective dynamical properties of a binary dusty plasma system. Our results constitute the first observation of the mode spectrum of a strongly coupled (liquid or solid) bilayer. Earlier results [23] were restricted to the weakly coupled state, where all collective modes exhibit an acoustic behavior. We confirm the predicted [7,8] benchmark of the strongly coupled mode structure, the development of optic modes with a wave number  $k = 0$  “energy (frequency) gap.”

Our dusty plasma experiments have been carried out in a custom designed vacuum chamber with an inner diameter of 25 cm and height of 18 cm, equipped with glass viewports, pressure meters, a turbomolecular pump, and a gas filling system. The lower, powered, 18 cm diameter, flat, horizontal, stainless steel electrode faces the upper, ring shaped, grounded aluminum electrode with an inner diameter of 15 cm at a height of 13 cm. Experiments have been performed in argon gas discharge at a pressure  $p = 0.8 \pm 0.05$  Pa, in a steady gas flow of  $\sim 0.01$  sccm, with 13.56 MHz radio frequency excitation of  $\sim 5$  W power. In the experiment melamine-formaldehyde microspheres with diameters  $d_1 = 3.63 \pm 0.06 \mu\text{m}$  and  $d_2 = 4.38 \pm 0.06 \mu\text{m}$  are used. For illumination we apply a

200 mW, 532 nm laser. Our CCD camera has a resolution of 1.4 megapixels and runs at 29.54 frames per second acquisition rate. Particle masses are  $m_1 = 3.8 \times 10^{-14}$  kg and  $m_2 = 6.6 \times 10^{-14}$  kg.

During the evaluation of the raw images ( $>60\,000$  per experiment) identification and position measurement of the particles is performed using the method described in [24]. The identification of the light and heavy (smaller and larger) particles is based on their scattered intensities, which is in this size domain proportional to the square of the diameter. After tracing the particles' motion from frame to frame we obtain the positions and velocities of each particle as a function of time. The layer separation was measured by tilting the camera and illuminating setup and taking images through the side window. After calibrating with a size standard we find the following average structural parameters: number of particles,  $N_1 = 682$ ,  $N_2 = 636$ ; the Wigner-Seitz radius calculated from the total number of the observed particles ( $N$ ) and the area ( $A$ ) of the field of view,  $a = \sqrt{A/\pi N} = 0.243$  mm, the layer separation is  $d/a = 0.43$ .

Based on the particle positions the  $g(r)$  pair-distribution function is obtained and compared to the results of molecular-dynamics (MD) simulation, as shown in Fig. 1. Experiment and simulation capture qualitatively identical features: order, shape, and position of the peaks agree satisfactorily. Differences in the amplitude and decay rate are due to different boundary conditions (confined versus periodic), friction, and charge fluctuations neglected in the simulation. Peak positions are consistent with the underlying hexagonal lattice structure, in agreement with theoretical results [7,12].

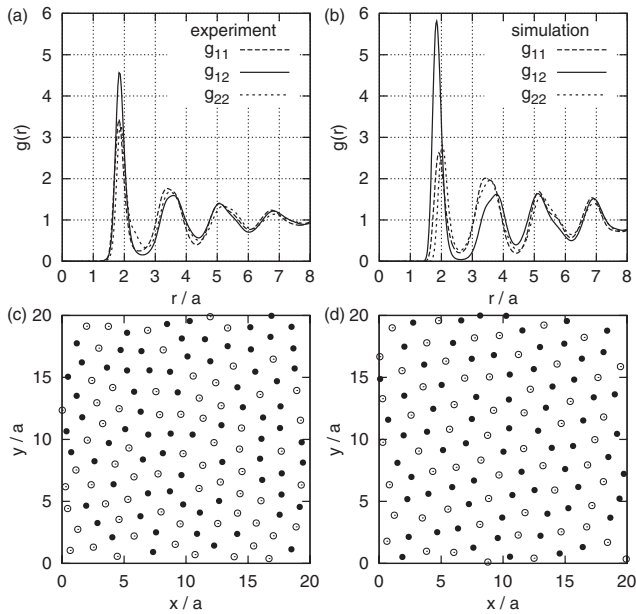


FIG. 1. Pair-distribution functions and particle snapshots obtained from the experiment (a),(c) and the MD simulation (b),(d). Indexes and symbol types label the layers (open, layer 1; filled, layer 2).

Although the ground state configuration for this bilayer is a regular staggered rectangular lattice, a large degree of substitutional disorder [25], due to the small interlayer separation and the finite temperature, was observed, as shown in the particle snapshots in Fig. 1.

In the MD simulation Yukawa-type pair interaction  $\Phi_{ij} = (e^2 Z_i Z_j / 4\pi\epsilon_0) \exp[-r_{ij}/\lambda_D] / r_{ij}$ , where  $r_{ij}$  is the three-dimensional distance between particles  $i$  and  $j$ , is assumed using  $\sim 4000$  particles with periodic boundary conditions. Since the interlayer separation is of the order of  $1/4\lambda_D$  (see below), the attractive force between grains in the two layers due to ion focusing or wakefield effects is assumed to be small, since these effects occur generally at larger separations (see, e.g., [26]). The neglect of such attractive forces is further bolstered by the experimental observation that the grains in the two layers do not form strings, but rather assume a staggered structure. Particle densities, masses, and layer separation are taken from the experiment,  $\kappa = a/\lambda_D = 0.5$  and  $Z_1 = 2550$ ,  $Z_2 = (d_2/d_1)Z_1 \approx 3080$  are further assumed; this parameter set was found in lattice calculations to best reproduce experimental dispersions.

In the experiment we observe a pressure jump of about 38% when switching on the discharge. Taking into account the active and the total volume of the vacuum system, this results in an  $\approx 85\%$  average temperature increase in the discharge region, resulting in  $T_{\text{gas}} \approx 550$  K. Measuring the dust particle velocities gives the direct kinetic energy, resulting in  $T_{v1} \approx 400$  K and  $T_{v2} \approx 500$  K for the two layers, and the Coulomb coupling parameters [defined as  $\Gamma_m = (e^2/4\pi\epsilon_0)(Z_m^2/k_B T_m a_m)$ ]:  $\Gamma_1 \approx 800$  and  $\Gamma_2 \approx 900$ . To obtain dynamical information on the system's collective excitations we use the method based on the Fourier transform of the microscopic density and current fluctuations, as in MD simulations [11,27]. Knowing the particle positions versus time, first we calculate the microscopic densities, as well as longitudinal and transverse currents:  $\rho^{(m)}(\mathbf{k}, t) = \sum_j \exp(-i\mathbf{k} \cdot \mathbf{r}_j)$ ,  $\lambda^{(m)}(\mathbf{k}, t) = \sum_j v_{j,\parallel} \exp(-i\mathbf{k} \cdot \mathbf{r}_j)$ ,  $\tau^{(m)}(\mathbf{k}, t) = \sum_j v_{j,\perp} \exp(-i\mathbf{k} \cdot \mathbf{r}_j)$  for the two layers ( $m = 1, 2$ ). From the Fourier transforms of  $\rho(\mathbf{k}, t) \rightarrow \rho(\mathbf{k}, \omega)$ ,  $\lambda \rightarrow \lambda(\mathbf{k}, \omega)$ , and  $\tau \rightarrow \tau(\mathbf{k}, \omega)$  we obtain the power spectra, e.g.,  $S_{m,n}(\mathbf{k}, \omega) \propto \langle \rho^{(m)}(-\mathbf{k}, -\omega) \rho^{(n)}(\mathbf{k}, \omega) \rangle$ , averaging is over the time slices available. In the present case of an asymmetric bilayer the labeling of the modes is not possible in a simple way, as it is for symmetric bilayers [11], where the two “+” and “-” polarizations clearly separate and correspond to in and out of phase oscillations. Therefore, in the following we do not label the modes, we only indicate in which spectra they appear as peaks. For an analysis of the mode structure one has to examine the spectra individually and identify the peak positions. Sample spectra are shown in Fig. 2 to illustrate the fundamental features in more detail. Plotted are results of the bilayer experiment and the MD simulation. As a reference standard, plotted are results of a separately performed single-layer experiment carried out in the same experimen-

tal setup and under the same conditions except for using only one particle species (with diameter  $4.38 \pm 0.06 \mu\text{m}$ , the total particle number in the field of view was  $N = 1945$ , resulting in higher density, thus higher nominal plasma frequency as in the bilayer case).

In Figs. 2(a) and 2(b) one can observe both in the experiment and in the simulation the presence of a strong primary peak at lower frequencies and a shoulderlike, weak and wide feature at higher ( $\omega \approx 50 \text{ s}^{-1}$ ) frequencies. The strength of this high-frequency peak becomes more obvious in comparison with the single-layer experiment, where at the same frequency the spectral power has already dropped 2 orders of magnitude, while it has the same slope as seen in the bilayer spectrum at higher frequencies ( $\omega > 70 \text{ s}^{-1}$ ). Figure 2(c) shows the interlayer density fluctuation spectrum  $S_{12}$  at  $ka = 0.4$  from the experiment and the MD simulation. The novel feature here is the appearance of a negative peak indicating an out of phase oscillation at the higher frequency, coinciding with the falloff point of the “shoulder” in the  $L_{11}$  and  $T_{11}$  spectra.

We compare our observational results with the mode dispersion calculated through two theoretical models. The first model is a perfect staggered rectangular lattice, with phonon propagation along the two principal axes. The lattice calculation is based on the formalism used in [7] for electronic bilayers, adopted to the asymmetric Yukawa

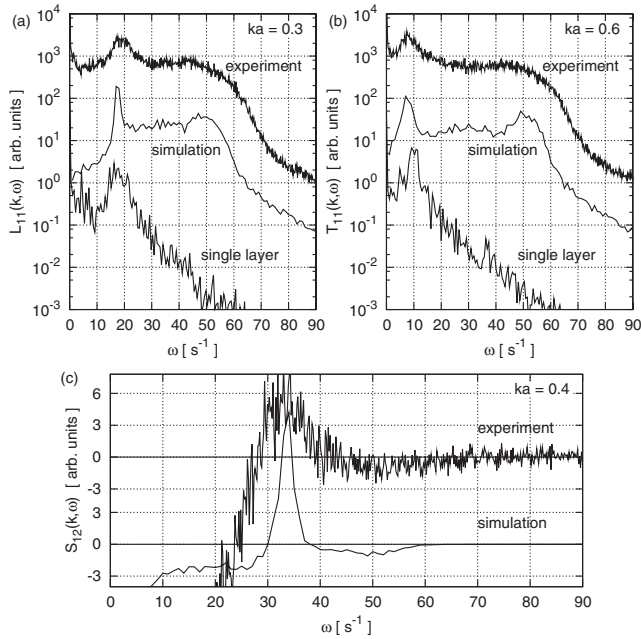


FIG. 2. Sample spectra illustrating the principal features of (a)  $L_{11}$  longitudinal, (b)  $T_{11}$  transverse current fluctuations, and (c)  $S_{12}$  interlayer density fluctuations. The one-layer spectra from the experiment and MD simulations are shown and compared to experimental single-layer spectra obtained in a separate measurement. The interlayer spectra (experiment and MD simulation) show a positive and a negative peak representing the in phase and out of phase oscillations, respectively. The vertical scale is shifted for clarity.

system. The second model is a completely disordered solid bilayer, with the mode dispersion calculated in the quasi-localized charge approximation (QLCA) formalism. The QLCA formalism was adapted to the binary Yukawa bilayer system (based on [28,29]) and the dispersions for the 4 modes were calculated with the input of the experimental pair-correlation functions. It should be noted that while for symmetric configurations the (in general)  $4 \times 4$  dynamical matrix can be decomposed into two  $2 \times 2$  matrices, resulting in a clear separation of the collective modes into longitudinal versus transverse and in phase versus out of phase polarizations, in the present case, this kind of mode separation, in general, is not possible. It can be derived only along the directions of the principal axes of the crystal, or in an approximation where the system is assumed to be isotropic as in the QLCA description.

Figure 3 shows an example of the longitudinal and transverse current fluctuation spectra measured without angular resolution in the upper layer. Overlaid are combined  $0^\circ$  and  $90^\circ$  lattice phonon [3(a) and 3(b)], and the (isotropic) QLCA mode dispersion curves [3(c) and 3(d)]. An additional, very low frequency, linear dispersion can be seen, which is most likely the footprint of an unavoidable net motion of the particle cloud.

Figure 4 shows the more detailed dispersion properties of the dusty plasma bilayer measured along a single direction together with lattice phonon results. The observed modes are not labeled, for reasons discussed above, only their sources (the spectra in which the peak was found) are indicated.

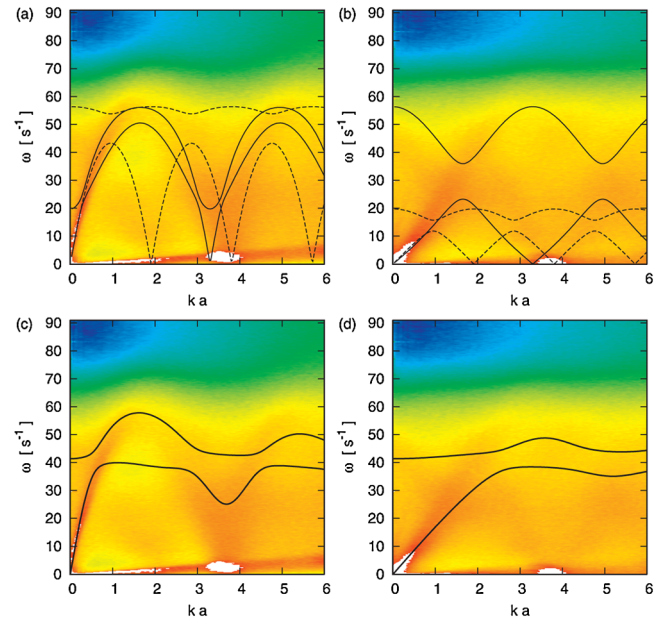


FIG. 3 (color online).  $L_{11}$  one-layer longitudinal (a),(c) and  $T_{11}$  one-layer transverse (b),(d) current fluctuation spectra. Peak positions [red (dark contours)] mark the dispersion  $\omega(k)$ . Black lines in (a),(b) are frequencies from lattice summation calculations including the two principal lattice directions. Lines in (c), (d) are the corresponding QLCA dispersions.

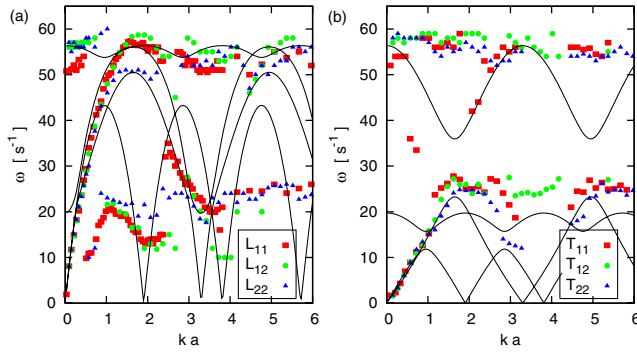


FIG. 4 (color online). Symbols: peaks identified in the longitudinal (a) and transverse (b) experimental spectra. Lines: selected lattice dispersions with  $x$  and  $y$  polarizations.

In Figs. 3 and 4 we observe the expected acoustic modes similar to those in 2D Yukawa layers. Figure 4 shows an additional prominent high-frequency ( $\omega \approx 55 \text{ s}^{-1}$ ) optical excitation together with the trace of a low-frequency ( $\omega \approx 25 \text{ s}^{-1}$ ) optical excitation. In Fig. 3 the angle averaged broad optical spectrum is observed, centered around  $\omega \approx 40 \text{ s}^{-1}$ . These observations are consistent with theoretical results for lattice phonons [7] and with QLCA [28] predictions for the so-called energy (frequency) gap in strongly coupled liquids or disordered systems, also studied in great detail in earlier MD simulations [8,11]. The QLCA model provides a value for the gap frequency, which, calculated with the input of experimental and simulation  $g_{12}(r)$  data, yields  $\omega_{\text{gap}}^{\text{exp}} = 41.4 \text{ s}^{-1}$  and  $\omega_{\text{gap}}^{\text{MD}} = 43.5 \text{ s}^{-1}$ .

In view of the prevailing local lattice structure in coexistence with a high degree of disorder, it is not *a priori* clear which of the two models (lattice versus QLCA) should provide a better description of the mode structure. Inspection of Fig. 3 shows that for low  $k$  values the acoustic portions of the low-frequency modes are equally well described by either model. For higher  $k$  values the repeated Brillouin zone structure is clearly visible. The optic frequency values in Fig. 4 are in the vicinity of the lattice frequencies. These features indicate the superiority of the lattice model. On the other hand, the QLCA predicted single “frequency gap” at  $k = 0$  lies in the center portion of the spectra in Fig. 3. This agreement and the high- $k$  tapering off of the optic modes seem to be more along the line of the QLCA description.

We can conclude that our dusty plasma experiment using two different dust sizes created a strongly coupled bilayer system that can be well approximated by a binary Yukawa bilayer model. This model has served as the basis for MD simulations, lattice calculations, and a QLCA calculation. All these approaches are in good agreement with the experiment, and verify the presence of an optical collective mode characterized by a finite energy (frequency) gap at  $k = 0$  wave number, distinguishing the strongly coupled bilayer from a weakly coupled one, where all the modes have an acoustic character.

Work partially supported by OTKA-PD-75113, OTKA-K-77653, MTA-NSF/102, NSF Grants PHY-0813153, PHY-0812956, PHY-0903808, DOE Grants DE-FG02-03ER54716, DE-FG02-04ER54804. This Letter was supported by the Janos Bolyai Research Grant of the Hungarian Academy of Sciences. Experimental setup was partially donated by the MOM-Szerviz Kft, and assembled by J. Forgács, J. Tóth, and Gy. Császár.

- [1] J. A. Seamons *et al.*, Phys. Rev. Lett. **102**, 026804 (2009).
- [2] T. B. Mitchell *et al.*, Science **282**, 1290 (1998).
- [3] E. B. Watkins *et al.*, Phys. Rev. Lett. **102**, 238101 (2009).
- [4] O. I. Yuzepovich *et al.*, Low Temp. Phys. **34**, 985 (2008).
- [5] S. Das Sarma and A. Madhukar, Phys. Rev. B **23**, 805 (1981); for more references, see [8(c)]
- [6] Yu. M. Vil'k and Yu. P. Monarkha, Sov. J. Low Temp. Phys. **11**, 535 (1985).
- [7] G. Goldoni and F. M. Peeters, Phys. Rev. B **53**, 4591 (1996).
- [8] (a) K. I. Golden and G. Kalman, Phys. Status Solidi B **180**, 533 (1993); (b) G. J. Kalman, Y. Ren, and K. I. Golden, Phys. Rev. B **50**, 2031 (1994); (c) G. J. Kalman, V. Valtchinov, and K. I. Golden, Phys. Rev. Lett. **82**, 3124 (1999).
- [9] I. V. Schweigert *et al.*, Phys. Rev. Lett. **82**, 5293 (1999).
- [10] Z. Donkó and G. J. Kalman, Phys. Rev. E **63**, 061504 (2001).
- [11] Z. Donkó *et al.*, Phys. Rev. Lett. **90**, 226804 (2003); Z. Donkó *et al.*, J. Phys. A **36**, 5877 (2003).
- [12] R. Messina and H. Löwen, Phys. Rev. Lett. **91**, 146101 (2003).
- [13] S. Ranganathan and R. E. Johnson, Phys. Rev. B **69**, 085310 (2004).
- [14] P. Hartmann *et al.*, Europhys. Lett. **72**, 396 (2005).
- [15] G. J. Kalman *et al.*, Phys. Rev. Lett. **98**, 236801 (2007).
- [16] S. Ranganathan and R. E. Johnson, Phys. Rev. B **75**, 155314 (2007).
- [17] A. Filinov *et al.*, J. Phys. Conf. Ser. **35**, 197 (2006).
- [18] S. De Palo *et al.*, Phys. Rev. Lett. **88**, 206401 (2002).
- [19] G. E. Astrakharchik, J. Boronat, I. L. Kurbakov, and Yu. E. Lozovik, Phys. Rev. Lett. **98**, 060405 (2007).
- [20] B. Smith, T. Hyde, L. Matthews, J. Reay, M. Cook, and J. Schmoke, Adv. Space Res. **41**, 1510 (2008).
- [21] L. S. Matthews, K. Qiao, and T. W. Hyde, Adv. Space Res. **38**, 2564 (2006).
- [22] S. Ranganathan and R. E. Johnson, Phys. Rev. B **78**, 195323 (2008).
- [23] D. S. Kainth *et al.*, J. Phys. Condens. Matter **12**, 439 (2000).
- [24] Y. Feng *et al.*, Rev. Sci. Instrum. **78**, 053704 (2007).
- [25] G. J. Kalman *et al.*, in *Condensed Matter Theories*, edited by J. Providencia and F. B. Malik (Nova Science, New York, 1998), Vol. 13, p. 203.
- [26] M. Lampe *et al.*, Phys. Plasmas **7**, 3851 (2000).
- [27] J. P. Hansen *et al.*, Phys. Rev. A **11**, 1025 (1975).
- [28] K. I. Golden and G. J. Kalman, Phys. Plasmas **7**, 14 (2000).
- [29] Z. Donkó *et al.*, in Proceedings of the 12th Workshop on the Physics of Dusty Plasmas, Boulder, CO, 2009, Abstracts of Contributed Papers (to be published).